

Statistical Modeling of Airborne Virus Transmission Through Imperfectly Fitted Face Masks

Sebastian Lotter, Lukas Brand, Maximilian Schäfer, and Robert Schober
Friedrich-Alexander University, Erlangen-Nuremberg, Germany
{sebastian.g.lotter,lukas.brand,max.schaefer,robert.schober}@fau.de

ABSTRACT

The rapid emergence and the disastrous impact of the severe acute respiratory syndrome coronavirus 2 (SARS-CoV-2) pandemic on public health, societies, and economies around the world has created an urgent need for understanding the pathways critical for virus transmission and counteracting the spread of SARS-CoV-2 efficiently. Airborne virus transmission by asymptomatic SARS-CoV-2-infected individuals is considered to be a major contributor to the fast spread of SARS-CoV-2 and social distancing and wearing of face masks in public have been implemented as countermeasures in many countries. Concerted research efforts in diverse scientific fields have meanwhile advanced the understanding of the physical principles of the manifold processes involved in airborne transmission of SARS-CoV-2. As part of these efforts, the physics and dynamics of aerosol filtration by various types of face masks have been studied. However, a comprehensive risk assessment framework for the airborne transmission of SARS-CoV-2 incorporating realistic assumptions on the filtration of infectious aerosols (IAs) by face masks is not available yet. In particular, in most end-to-end models for airborne virus transmission, it is neglected that the stochastic spread of IAs through imperfectly fitted face masks depends on the dynamics of the breathing of the wearer. In this paper, we consider airborne virus transmission from an infected but asymptomatic individual to a healthy individual, both wearing imperfectly fitted face masks, in an indoor environment. By framing the end-to-end virus transmission as a Molecular Communications (MC) system, we obtain a statistical description of the number of IAs inhaled by the healthy person subject to the respective configurations of the face masks of both persons. We demonstrate that the exhalation and inhalation air flow dynamics have a significant impact on the stochastic filtering of IAs by the imperfectly fitted face masks. Furthermore, we are able to show that the fit of the face mask of the infected person can highly impact the infection probability if the infectious dose for virus transmission to the healthy person is in a critical range. We conclude that the proposed MC model may contribute a valuable assessment tool to fight the spread of SARS-CoV-2 as it naturally encompasses the randomness of the transmission process and thus enables comprehensive risk analysis beyond statistical averages.

1 INTRODUCTION

The global outbreak of the *coronavirus disease 2019 (COVID-19)* [26] since fall 2019 has impacted and is impacting societies all over the world causing large-scale and long-term damage to public health, society, and economy. COVID-19 is caused by a novel type of coronavirus, *severe acute respiratory syndrome coronavirus 2 (SARS-CoV-2)*, which is highly transmissible between humans [11]. To contain the

spread of SARS-CoV-2, it has soon been advocated to target the airborne transmission of SARS-CoV-2 in indoor environments, since this transmission route is expected to contribute significantly to the spread of the virus [1, 19]. Airborne viral transmission in *poorly ventilated* indoor environments by *asymptomatic* individuals is especially relevant, because, in the absence of proper ventilation, the infectious aerosols (IAs), i.e., the virus carrying microdroplets, possibly remain suspended in the room air for a long time and asymptomatic individuals have no indication to quarantine themselves [16]. To minimize the risk of airborne transmission of SARS-CoV-2, face masks have been widely and successfully used in practice [8]. At the same time, experts with diverse professional backgrounds have studied the impact of face masks on the airborne transmission of SARS-CoV-2 experimentally and in modeling studies [10]. While these efforts have advanced the scientific understanding of many processes and parameters relevant for airborne virus transmission, a comprehensive assessment of the impact of face masks on the infection risk remains challenging. Specifically, the end-to-end modeling of airborne SARS-CoV-2 transmission starting with the exhalation of IAs by an infected person (IP) and ending with the inhalation of IAs by a healthy person (HP) is complicated by the inherent randomness of the process. This randomness originates from the small number of IAs typically involved in virus transmission [5] and it implies that a statistical characterization of the transmission (beyond the mean) is required to fully assess the infection risk. However, existing transmission models tend to neglect this randomness in favor of a comprehensible mathematical model and communicable outcomes [17]. Additional randomness arises if the face mask is not fitted perfectly to the face of the wearer. In this case, part of the breathing airflow and, consequently, some of the exhaled IAs do not pass the mask filter piece but leak through gaps at the edge of the mask. This leakage flow has been attributed significance for airborne virus transmission [25] and needs therefore to be accounted for. However, in existing end-to-end models for airborne virus transmission, it is often not taken into account. In order to overcome these limitations, in this paper, we explore the modeling of airborne virus transmission under the framework of Molecular Communications (MC), an interdisciplinary research field that has recently emerged at the intersection of information and communication theory and biology [20].

The MC paradigm has been applied to model airborne virus transmission in [7, 9, 12, 13, 24]. However, the impact of face masks on the statistics of the end-to-end airborne virus transmission has not been considered. In a recent overview paper [2], a perspective on future directions in applying MC to viral infection research is given. Finally, in [14], the SARS-CoV-2 transmission within the human respiratory tract is modeled using MC.

In contrast to existing papers using MC to study airborne virus transmission, we propose a novel model for airborne virus transmission via IAs that takes into account the randomness introduced by imperfectly fitted face masks. Hence, in contrast to existing models, the model proposed in this paper allows for a comprehensive assessment of the infection risk imposed by imperfectly fitted face masks. By numerical evaluation, we are able to show the impact of the physical face mask parameters on the infection probability of a HP exposed to IAs emitted by an asymptomatic, regularly breathing IP. We further show the impact of the different breathing dynamics during exhalation and inhalation, respectively, on the stochastic filtering of IAs by the face mask. Despite its simplicity, the proposed model generates insight into the statistics of the indoor transmission of SARS-CoV-2 from an infected, but asymptomatic person to a susceptible person both protected by imperfectly fitted face masks.

The remainder of this paper is organized as follows. In Section 2, we introduce the considered physical virus transmission scenario. In Sections 3, 4, and 5, we present the transmitter, channel, and receiver models, respectively, required for framing airborne virus transmission as MC system. In Section 6, we present results from the numerical evaluation of the proposed model, before we summarize our main findings in Section 7.

2 PHYSICAL TRANSMISSION SCENARIO

We consider a generic closed indoor environment with one HP present. Another person which is infected but asymptomatic, i.e., the IP, is present in the room for T_{tot} seconds. After T_{tot} seconds, the IP leaves the room. The HP is present in the room while the IP is present and stays in the room after the IP has left. Both the IP and the HP breath regularly while they are present in the room. While breathing, the IP exhales virus-carrying aerosols, i.e., the IAs¹.

Both the IP and the HP wear face masks. However, the masks do not act as perfect filters for the IAs, because

- the face mask fabric does not block all IAs [17] and
- the fit of the face masks to the faces of the IP and the HP, respectively, is not perfect, such that IAs possibly pass through gaps between the edge of the face mask and the skin during breathing [15].

When the IP exhales, some of the viruses present in his respiratory tract dissolve in the exhalation air as IAs [18]. Upon exhalation, some of these IAs deposit in the face mask of the IP, some are released into the ambient air. The exhaled IAs that did not deposit in the face mask of the IP spread in the room due to the turbulent ambient air flow [18]. Ultimately, each emitted IA either deposits on a surface in the room or on the face mask of the IP or the HP, respectively, degrades with a rate depending on the room temperature and relative humidity, or is inhaled by the HP or the IP [16].

In order to study the exposure of the HP to IAs released by the IP, we frame the airborne transmission scenario outlined above as MC system, cf. Fig.1. To this end, we consider the IP as molecular transmitter, the HP as molecular receiver, and the room as channel. In this system model, information is conveyed from the IP to the

¹In general, the exhalation air contains aerosols of different sizes, some of which carry viruses and some of which do not. In this paper, we restrict our attention to small (average diameter 5 μm), virus-carrying aerosols that remain dissolved in air for up to 2.6 hours [16].

HP by the release of signaling molecules in the form of IAs into the channel. The HP repeatedly samples the IA concentration in the environment by inhaling aerosols and accumulates the inhaled IAs in his respiratory tract. If the cumulative number of inhaled IAs exceeds some threshold, the HP gets infected, i.e., the virus has been transmitted from the IP to the HP.

Due to the impact of several random parameters such as the ambient air flow, the room temperature, and the air humidity on the propagation and degradation of IAs [18], the virus transmission is random. Furthermore, the face masks of the IP and the HP, respectively, render the release and the inhalation of the IAs random, as some of the IAs are filtered by the masks. In the following sections, we present models for the transmitter, the channel, and the receiver, respectively, that encompass this randomness and finally allow us to evaluate the statistics of the number of IAs inhaled by the HP.

3 TRANSMITTER

In the considered airborne virus transmission system, cf. Section 2, virions deposited in the respiratory tract of the IP dissolve in the exhalation air flow and are transported as IAs through the IP's mouth/nose. After leaving the mouth/nose of the IP, the IAs are either filtered by the face mask of the IP (and not further considered in our model) or emitted into the environment (physical channel). Hence, the molecular transmitter in our model involves three sequential stages:

- Generation of solute IAs within the respiratory tract during exhalation
- Exhalation of IAs through the mouth/nose into the volume enclosed by the face mask and the face of the IP
- Deposition of IAs in the face mask or release into the environment

3.1 Number of Exhaled Infectious Aerosols

We assume that the IP stays in the room for T_{tot} seconds. For simplicity, we also assume that T_{tot} is an integer multiple of T , i.e., $T_{\text{tot}}/T = I \in \mathbb{N}$, where \mathbb{N} denotes the set of positive integers and I denotes the number of breaths that the IP takes in the room. For each interval $i \in \{1, \dots, I\}$, we denote the number of exhaled IAs in i by N_i . According to [5], N_i follows a Poisson distribution with mean λ , i.e., $N_i \sim \text{Pois}(\lambda)$, and, according to empirical observations, λ ranges from 0.0000000049 virus copies per cm^3 for low emitters to 0.637 virus copies per cm^3 for high emitters infected with COVID-19 [22]. Finally, we denote the set of IAs exhaled during T_{tot} as $\mathcal{M} = \{M_1, \dots, M_J\}$, where $J = \sum_{i=1}^I N_i$. Since the N_i are independent Poisson random variables (RVs) with identical mean λ , J is a Poisson RV with mean λI , i.e., $J \sim \text{Pois}(\lambda I)$.

3.2 Exhalation Model

We assume that the regular breathing of the IP follows the experimentally obtained breathing pattern reported in [15, 23]. In this model, one breath consists of one exhalation followed by one inhalation and regular breathing is a sequence of identical breaths. This means that each breath in such a sequence of breaths is identical with respect to its total duration and the relative duration of exhalation and inhalation. Let T denote the length of one breath in seconds. Let further denote t_j^{lx} , $j \in \{1, \dots, J\}$, the time variable

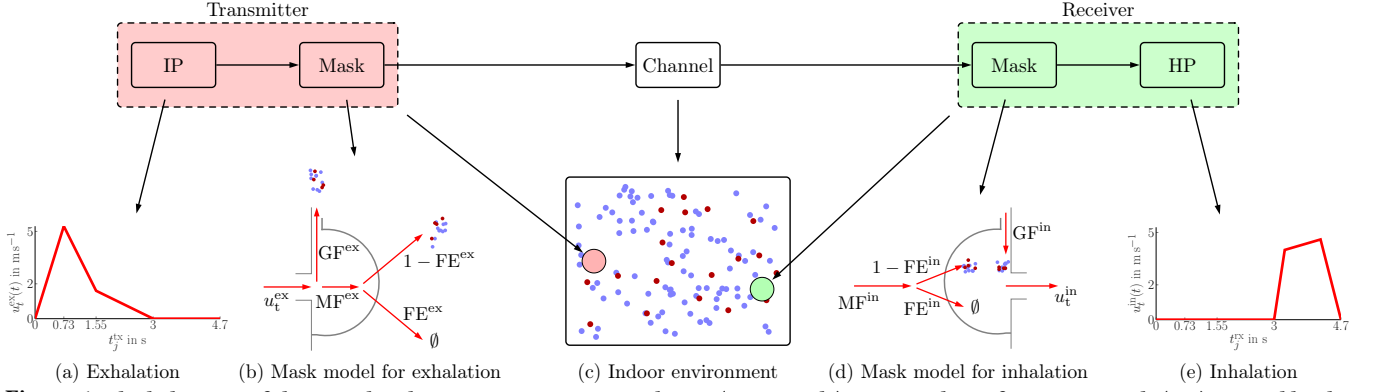


Figure 1: Block diagram of the considered transmission scenario: The HP (green circle) is exposed to infectious aerosols (IAs) emitted by the IP (red circle) in an indoor environment. The IP breathes regularly and emits aerosols during exhalation (a), which can in general be non-infectious (blue dots) or infectious (red dots). While we consider only IAs in this paper, the non-infectious aerosols are included in this figure to show the relative abundance of non-infectious aerosols as compared to IAs in the exhaled air of the IP [5]. Exhaled aerosols are emitted into the environment as part of the exhalation mask flow MF^{ex} through the face mask of the IP or as part of the (unfiltered) exhalation gap flow GF^{ex} (b). The HP breathes regularly and inhales (e) air. IAs captured by the inhalation air flow of the HP are either part of the inhalation mask flow MF^{in} or part of the (unfiltered) inhalation gap flow GF^{in} (d).

ranging over the interval $i \in \{1, \dots, I\}$ in which IA j is exhaled relative to the beginning of this interval, i.e., $t_j^{\text{tx}} \in [0, T]$. For regular breathing, $T = 4.7$ s according to [15, 23]. Hence, during breath i of the IP, the absolute velocity of the exhalation air flow, $u_t^{\text{ex}}(t_j^{\text{tx}})$ in m s^{-1} , is then given by [15, 23]

$$u_t^{\text{ex}}(t_j^{\text{tx}}) = \begin{cases} 0, & 0 \leq t_j^{\text{tx}} < 0.73 \text{ s}, \\ \frac{5.3}{0.73} \frac{\text{m}}{\text{s}^2} t_j^{\text{tx}}, & 0.73 \text{ s} \leq t_j^{\text{tx}} < 1.55 \text{ s}, \\ \frac{(1.6-5.3)}{(1.55-0.73)} \frac{\text{m}}{\text{s}^2} (t_j^{\text{tx}} - 0.73 \text{ s}) + 5.3 \frac{\text{m}}{\text{s}}, & 1.55 \text{ s} \leq t_j^{\text{tx}} < 3 \text{ s}, \\ \frac{-1.6}{(3-1.55)} \frac{\text{m}}{\text{s}^2} (t_j^{\text{tx}} - 1.55 \text{ s}) + 1.6 \frac{\text{m}}{\text{s}}, & 3 \text{ s} \leq t_j^{\text{tx}} < 4.7 \text{ s}. \end{cases} \quad (1)$$

According to (1), $u_t^{\text{ex}}(t_j^{\text{tx}})$ is a piecewise linear function defined for $t_j^{\text{tx}} \in [0, T]$. Fig. 1(a) shows $u_t^{\text{ex}}(t_j^{\text{tx}})$ as defined in (1).

3.3 Exhalation Time

After an IA M_j , $j \in \{1, \dots, J\}$, has been exhaled in interval i , it is either captured by the face mask of the IP or released into the room. We recall from Section 2 that the face mask is imperfectly fitted to the face of the IP and, hence, some of the exhaled aerosols leak through gaps between the face mask and the skin without passing through the mask fabric. This leakage flow, in turn, depends on the velocity of the exhalation air flow [21] at the time at which M_j is exhaled. Now, assuming that IAs are uniformly distributed over the total volume of air exhaled in breath i , the probability that M_j is exhaled in any sub-interval of this breath is proportional to the exhalation air flow rate, i.e.,

$$\Pr\{T_j^{\text{ex}} \leq t_j^{\text{tx}}\} = \frac{\int_0^{t_j^{\text{tx}}} F_t^{\text{ex}}(\tau) d\tau}{\int_0^T F_t^{\text{ex}}(\tau) d\tau} = \frac{\int_0^{t_j^{\text{tx}}} u_t^{\text{ex}}(\tau) d\tau}{\int_0^T u_t^{\text{ex}}(\tau) d\tau}, \quad 0 \leq t_j^{\text{tx}} \leq T, \quad (2)$$

where T_j^{ex} denotes the random time of exhalation of M_j relative to the beginning of breath i and $F_t^{\text{ex}}(t_j^{\text{tx}})$ denotes the total flow rate of exhaled air in $\text{m}^3 \text{s}^{-1}$ at t_j^{tx} , i.e., $F_t^{\text{ex}}(t_j^{\text{tx}}) = u_t^{\text{ex}}(t_j^{\text{tx}}) S_t^{\text{tx}}$, where S_t^{tx} denotes the surface area of the mouth/nose of the IP in m^2 .

According to (2), $\Pr\{T_j \leq t_j^{\text{tx}}\}$ can be obtained by integrating (1) (which is straightforward).

3.4 Escape Probability

To account for the imperfect fit of the face mask of the IP, we distinguish the air flows through the face mask and through the gaps at the edge of the mask during exhalation and call them *exhalation mask flow* (MF^{ex}) and *exhalation gap flow* (GF^{ex}), respectively. To characterize MF^{ex} and GF^{ex} , we adopt the analytical fluid dynamics model for the breathing of a person through a face mask from [21]. In this simplified model, the face area around the mouth/nose of the person is modeled as a planar surface, the face mask is modeled as a half-sphere, and the gaps are modeled as one cuboid extending from the surface of the mask towards the environment, see Fig. 1(b) for a schematic representation of the model and [21, Fig. 1] for details. The model from [21] quantifies MF^{ex} and GF^{ex} as functions of various parameters of the face mask and the exhaled air flow rate. Furthermore, it has been validated by three-dimensional fluid dynamics simulation in [21].

Let $F_g^{\text{ex}}(t)$ denote the air flow rate through the gaps at the edge of the face mask of the IP in $\text{m}^3 \text{s}^{-1}$ at time t , $0 \leq t \leq T$. According to [21] and assuming spatially uniform air pressure within the volume enclosed by the face mask and the skin of the IP at any time t , $F_g^{\text{ex}}(t)$ is given by [21]

$$F_g^{\text{ex}}(t) = u_g^{\text{ex}}(t) H_g^{\text{tx}} B_g^{\text{tx}}, \quad (3)$$

where H_g^{tx} and B_g^{tx} denote the height and the width, respectively, of the gap in m and $u_g^{\text{ex}}(t)$ is given by [21]

$$u_g^{\text{ex}}(t) = \frac{1}{\zeta \rho} \left[- \left(\frac{12\mu L_g^{\text{tx}}}{(H_g^{\text{tx}})^2} + \frac{C_m^{\text{tx}} \rho H_g^{\text{tx}} B_g^{\text{tx}}}{S_m^{\text{tx}}} \right) + \sqrt{\left(\frac{12\mu L_g^{\text{tx}}}{(H_g^{\text{tx}})^2} + \frac{C_m^{\text{tx}} \rho H_g^{\text{tx}} B_g^{\text{tx}}}{S_m^{\text{tx}}} \right)^2 + 2 \frac{\zeta \rho^2 C_m^{\text{tx}} F_t^{\text{ex}}(t)}{S_m^{\text{tx}}}} \right], \quad (4)$$

where the constants L_g^{tx} , C_m^{tx} , S_m^{tx} , ζ , μ , and ρ denote the length of the gap in m, the viscous porous resistance of the face mask of the IP in m s^{-1} , the surface area of the face mask of the IP in m^2 , the pressure loss coefficient at the gap in kg m^{-1} , the dynamic viscosity of air in Pa s , and the density of air in kg m^{-3} , respectively. Hence, L_g^{tx} depends on the fit of the mask to the face of the IP, C_m^{tx} and S_m^{tx} are properties of the face mask of the IP, and ζ , μ , and ρ are physical constants.

From (3) and F_t^{ex} , we determine the probability that M_j , exhaled at time T_j^{ex} , escapes through the gap as

$$\Pr\{M_j \in \text{GF}^{\text{ex}}\} = \frac{F_g^{\text{ex}}(T_j^{\text{ex}})}{F_t^{\text{ex}}(T_j^{\text{ex}})} = 1 - \Pr\{M_j \in \text{MF}^{\text{ex}}\}. \quad (5)$$

If IA M_j instead is carried by the mask flow MF^{ex} , it deposits in the mask with a probability corresponding to the outward filtration efficiency of the mask, FE^{ex} , and passes the mask unfiltered with probability $1 - \text{FE}^{\text{ex}}$ [17]. Hence, the emission of M_j into the environment can be modeled as a Bernoulli RV $S_j^{\text{tx}} \in \{0, 1\}$, with probabilities

$$\begin{aligned} \Pr\{S_j^{\text{tx}} = 1\} &= 1 - \Pr\{S_j^{\text{tx}} = 0\} \\ &= \Pr\{M_j \in \text{GF}^{\text{ex}}\} + \Pr\{M_j \in \text{MF}^{\text{ex}}\}(1 - \text{FE}^{\text{ex}}), \end{aligned} \quad (6)$$

where $S_j^{\text{tx}} = 1$ and $S_j^{\text{tx}} = 0$ denote the events that M_j is emitted into the environment and M_j is filtered by the mask, respectively.

Finally, the total number of IAs emitted into the environment by the IP is given by

$$\text{EIA} = \sum_{j=1}^J S_j^{\text{tx}}, \quad (7)$$

$\text{EIA} \in \{0, \dots, J\}$, and we denote the emitted IAs by E_k , $k \in \{k_1, \dots, k_{\text{EIA}}\} \subseteq \{1, \dots, J\}$. According to (7), the discrete RV EIA is the sum of J independent Bernoulli RVs with different success probabilities depending on the random exhalation times of IAs M_j . If the ratio of the flow rates of GF^{ex} and MF^{ex} was constant with respect to time, i.e., $F_g^{\text{ex}}(t_1)/F_t^{\text{ex}}(t_1) = F_g^{\text{ex}}(t_2)/F_t^{\text{ex}}(t_2) = q$, for all $t_1, t_2 \in [0, T_j^{\text{ex}}]$, EIA would be a binomial distributed RV with success probability q . However, due to the nonlinear relationship between $F_g^{\text{ex}}(t)$ and $F_t^{\text{ex}}(t)$ in (3), (4), this is not the case.

4 CHANNEL

According to Section 2, after an IA E_k is emitted into the environment by the IP, it is subject to the turbulent flow of the ambient air before it either deposits on a surface, for example on a wall or on furniture, or is inhaled by either the IP or the HP. According to [17], the probability that E_k arrives at the HP in a viable, i.e., infectious, state can be written as the product of two probabilities, $p_a p_v$, where $p_a \in [0, 1]$ denotes the probability that E_k reaches the HP and $p_v \in [0, 1]$ denotes the probability that the virion carried by the aerosol is still infectious when reaching the HP. Depending on the room geometry, furniture, ventilation, and the positions of the IP and the HP in the room, p_a can be estimated using tools from fluid mechanics [3]. p_v depends on environmental conditions such as the relative humidity and temperature, on the travel time from the IP to the HP, and on the half-time of SARS-CoV-2 virions on aerosols [17]. Now we define the Bernoulli RV $S_k^{\text{ch}} \in \{0, 1\}$ to indicate whether E_k reaches the HP in a viable state and, recalling

that we have assumed that E_k did not deposit in the face mask of the IP during exhalation, we obtain

$$\Pr\{S_k^{\text{ch}} = 1 | S_k^{\text{tx}} = 1\} = p_a p_v = 1 - \Pr\{S_k^{\text{ch}} = 0 | S_k^{\text{tx}} = 1\}, \quad (8)$$

where $S_k^{\text{ch}} = 1$ and $S_k^{\text{ch}} = 0$ denote the events that E_k is captured and not captured by the inhalation air flow of the HP in a viable state, respectively, and $p_a p_v$ is identical for all IAs. Hence, without making any further assumptions on the room geometry, ventilation, and other properties of the physical environment, the propagation of E_k from the IP to the HP is modeled as Bernoulli RV². Due to the block-based approach used in this paper (see Fig. 1), more detailed propagation models can be readily adopted. While this is certainly an interesting extension to the model proposed in this paper, due to the space constraints, this is left for future work.

5 RECEIVER

In this section, we present a detailed model for the inhalation of IAs by the HP given that the HP wears an imperfectly fitted face mask that filters part of the aerosols from the inhaled ambient air. The presented model parallels in part the model presented in Section 3.

5.1 Inhalation Model

Analogously to Section 3, let $t_j^{\text{rx}} \in [0, T]$ denote the time variable ranging over the interval in which IA j is captured by the inhalation air flow of the HP (this does not imply that j is actually *inhaled* by the HP, as there is still a chance that it deposits in the HP's face mask) *relative to the beginning* of this interval, i.e., $t_j^{\text{rx}} \in [0, T]$. The inhalation of the HP in this interval is described by the time-dependent inhalation air flow velocity $u_t^{\text{in}}(t_j^{\text{rx}})$ in m s^{-1} given by [15, 23]

$$u_t^{\text{in}}(t_j^{\text{rx}}) = \begin{cases} 0 \frac{\text{m}}{\text{s}}, & 0 \text{ s} \leq t_j^{\text{rx}} < 3 \text{ s}, \\ \frac{4}{(3.27-3)} \frac{\text{m}}{\text{s}^2} (t_j^{\text{rx}} - 3 \text{ s}), & 3 \text{ s} \leq t_j^{\text{rx}} < 3.27 \text{ s}, \\ \frac{(4.6-4)}{(4.18-3.27)} \frac{\text{m}}{\text{s}^2} (t_j^{\text{rx}} - 3.27 \text{ s}) + 4 \frac{\text{m}}{\text{s}}, & 3.27 \text{ s} \leq t_j^{\text{rx}} < 4.18 \text{ s}, \\ \frac{-4.6}{(4.7-4.18)} \frac{\text{m}}{\text{s}^2} (t_j^{\text{rx}} - 4.18 \text{ s}) + 4.6 \frac{\text{m}}{\text{s}}, & 4.18 \text{ s} \leq t_j^{\text{rx}} < 4.7 \text{ s}. \end{cases} \quad (9)$$

Eq. (9) is illustrated in Fig. 1(e)³.

5.2 Inhalation Time

We assume that the IA E_k reaches the HP in a viable state according to the definition in Section 4, i.e., $S_k^{\text{ch}} = 1$. Then, the probability that E_k is carried by the inhalation air flow towards the respiratory tract of the HP at any random time $T_k^{\text{in}} \in [0, T]$ is proportional to the inhalation air flow, i.e.,

$$\Pr\{T_k^{\text{in}} \leq t_j^{\text{rx}}\} = \frac{\int_0^{t_j^{\text{rx}}} F_t^{\text{in}}(\tau) d\tau}{\int_0^T F_t^{\text{in}}(\tau) d\tau} = \frac{\int_0^{t_j^{\text{rx}}} u_t^{\text{in}}(\tau) d\tau}{\int_0^T u_t^{\text{in}}(\tau) d\tau}, \quad 0 \leq t_j^{\text{rx}} \leq T, \quad (10)$$

²Modeling molecule propagation as Bernoulli RV has been suggested in the context of airborne virus transmission [17] and has also been successfully applied in the context of MC [4].

³Note that we do not assume that the IP and the HP start breathing at the same time.

where the total inhalation air flow rate at time $t_j^{\text{rx}}, F_t^{\text{in}}(t_j^{\text{rx}})$ in $\text{m}^3 \text{s}^{-1}$, is defined as

$$F_t^{\text{in}}(t_j^{\text{rx}}) = u_t^{\text{in}}(t_j^{\text{rx}})S_t^{\text{rx}}, \quad (11)$$

where S_t^{rx} denotes the surface area of the mouth/nose of HP in m^2 .

5.3 Inhalation Mask Flow and Gap Flow

Since the HP, similar to the IP, wears an imperfectly fitted face mask, the air flow resulting from the inhalation of the HP is split into a mask flow component (MF^{in}) and a gap flow component (GF^{in}). To model MF^{in} and GF^{in} , as in Section 3, we adopt the fluid dynamics model from [21]. When an IA E_k reaches the HP, it follows the GF^{in} with a probability proportional to the flow through the gap relative to the total inhalation flow at time T_k^{in} , i.e.,

$$\Pr\{E_k \in \text{GF}^{\text{in}}\} = \frac{F_g^{\text{in}}(T_k^{\text{in}})}{F_t^{\text{in}}(T_k^{\text{in}})} = 1 - \Pr\{E_k \in \text{MF}^{\text{in}}\}, \quad (12)$$

where the air flow through the gap at time $t \in [0, T]$, $F_g^{\text{in}}(t)$ in $\text{m}^3 \text{s}^{-1}$, is defined as

$$F_g^{\text{in}}(t) = u_g^{\text{in}}(t)H_g^{\text{rx}}B_g^{\text{rx}}, \quad (13)$$

where H_g^{rx} and B_g^{rx} denote the height and the width of the gap between the face mask and the skin of the HP in m, respectively. The flow velocity of the gap flow, $u_g^{\text{in}}(t)$ in m s^{-1} is given by [21]

$$u_g^{\text{in}}(t) = \frac{1}{\zeta\rho} \left[- \left(\frac{12\mu L_g^{\text{rx}}}{(H_g^{\text{rx}})^2} + \frac{C_m^{\text{rx}}\rho H_g^{\text{rx}}B_g^{\text{rx}}}{S_m^{\text{rx}}} \right) + \sqrt{\left(\frac{12\mu L_g^{\text{rx}}}{(H_g^{\text{rx}})^2} + \frac{C_m^{\text{rx}}\rho H_g^{\text{rx}}B_g^{\text{rx}}}{S_m^{\text{rx}}} \right)^2 - 2 \frac{\zeta\rho^2 C_m^{\text{rx}} F_t^{\text{in}}(t)}{S_m^{\text{rx}}}} \right]. \quad (14)$$

Analogous to Section 3.4, the constants L_g^{rx} , C_m^{rx} , and S_m^{rx} denote the length of the gap in m, the viscous porous resistance of the HP's face mask in m s^{-1} , and the surface area of the HP's face mask in m^2 , respectively, and ζ , μ , and ρ are defined in Section 3.4. Eq. (12) follows from the observation that every inhaled aerosol is either part of GF^{in} or MF^{in} .

5.4 Inhalation Probability

With the observations from the previous section, we are able to determine the probability for any IA E_k reaching the HP at time T_k^{in} to actually pass the face mask and reach the respiratory tract of the HP. Similar to Section 3.4, we model the inhalation of E_k as a binary RV $S_k^{\text{rx}} \in \{0, 1\}$, where $S_k^{\text{rx}} = 1$ and $S_k^{\text{rx}} = 0$ denote the events that E_k is inhaled by the HP and E_k is filtered by the face mask of the HP, respectively. Now, $S_k^{\text{rx}} = 1$ if and only if E_k is part of GF^{in} or E_k is part of MF^{in} and not filtered by the face mask. Then, recalling that we have assumed that E_k did not deposit in the face mask of IP and reached HP, we obtain

$$\begin{aligned} \Pr\{S_k^{\text{rx}} = 1 | S_k^{\text{tx}} = 1, S_k^{\text{ch}} = 1\} \\ &= 1 - \Pr\{S_k^{\text{rx}} = 0 | S_k^{\text{tx}} = 1, S_k^{\text{ch}} = 1\} \\ &= \Pr\{E_k \in \text{GF}^{\text{in}}\} + \Pr\{E_k \in \text{MF}^{\text{in}}\}(1 - \text{FE}^{\text{in}}), \end{aligned} \quad (15)$$

and FE^{in} is the inward filtration efficiency of the face mask of the HP.

5.5 Detection

Let the binary RV S_j denote the event that IA j is transmitted from IP to HP via airborne transmission, i.e., $S_j = 1$ if IA j is transmitted and $S_j = 0$ otherwise. According to the results presented in the previous sections, we can write S_j as

$$S_j = S_j^{\text{tx}} S_j^{\text{ch}} S_j^{\text{rx}}, \quad (16)$$

where

$$\begin{aligned} \Pr\{S_j = 1\} &= \Pr\{S_j^{\text{tx}} = 1, S_j^{\text{ch}} = 1, S_j^{\text{rx}} = 1\} \\ &= \Pr\{S_j^{\text{tx}} = 1\} \Pr\{S_j^{\text{ch}} = 1 | S_j^{\text{tx}} = 1\} \times \\ &\quad \times \Pr\{S_j^{\text{rx}} = 1 | S_j^{\text{tx}} = 1, S_j^{\text{ch}} = 1\} \\ &= 1 - \Pr\{S_j = 0\}. \end{aligned} \quad (17)$$

The random number of inhaled IAs by HP, IIA , is given by

$$\text{IIA} = \sum_{j=1}^J S_j. \quad (18)$$

According to (18), IIA is a discrete random variable with support \mathbb{N}_0 , where \mathbb{N}_0 denotes the set of non-negative integers. Note that the S_j are independent Bernoulli RVs, but they are not identically distributed due to their dependence on the random exhalation and inhalation times of each IA, respectively. Hence, IIA does in general not follow a Binomial distribution.

According to commonly used models for virus transmission, HP gets infected if IIA reaches the infectious dose θ , $\theta \in \mathbb{N}_0$, that depends on the physical state and the state of the immune system of the HP [17]. Hence, the virus is transmitted from IP to HP with probability $P(\theta)$, where

$$P(\theta) = \Pr\{\text{IIA} \geq \theta\} = 1 - \sum_{n=0}^{\theta-1} \Pr\{\text{IIA} = n\}. \quad (19)$$

We refer to $P(\theta)$ as *infection probability*.

6 NUMERICAL RESULTS

In this section, we present numerical results for the MC based airborne virus transmission model presented in Sections 3, 4, and 5. To this end, we first describe our simulation framework and the parameters used. Then, we study the impact of some of these parameters on the end-to-end system.

6.1 Simulation and Choice of Parameters

To simulate the transmission scenario described in Sections 3, 4, and 5, we first computed the random number of exhaled IAs, J , according to Section 3.1. Next, we simulated the transmission of each of the J IAs from IP to HP as a sequence of random experiments according to (16). To this end, we first computed the random exhalation and inhalation times for each IA using inverse transform sampling [6] after integrating and inverting (2) and (10). Then, we used (16) to determine for each of the J exhaled IAs whether it was inhaled by the HP or not and finally summed up the inhaled IAs to obtain the random number of inhaled infectious aerosols, IIA , according to (18). We repeated this procedure 10,000 times to obtain the empirical distribution of the RV IIA as presented in the following sections. Table 1 lists the default simulation parameters.

Table 1: Default Simulation Parameters.

Parameter	Default Value	Description	Ref.
$H_g^{\text{tx}}, H_g^{\text{rx}}$	1×10^{-3} m	Face mask gap height	[21]
$B_g^{\text{tx}}, B_g^{\text{rx}}$	2.5×10^{-2} m	Face mask gap width	[21]
$L_g^{\text{tx}}, L_g^{\text{rx}}$	7.1×10^{-3} m	Face mask gap length	[21]
$C_m^{\text{tx}}, C_m^{\text{rx}}$	2×10^3 m s ⁻¹	Face mask viscous porous resistance	[21]
$S_m^{\text{tx}}, S_m^{\text{rx}}$	1.58×10^{-2} m ²	Face mask surface area	[21]
$S_t^{\text{tx}}, S_t^{\text{rx}}$	1×10^{-4} m ²	Respiratory tract surface area	[21]
$FE^{\text{ex}}, FE^{\text{in}}$	0.95	Face mask filtration efficiency	
ζ	1.5 kg m ⁻¹	Pressure loss coefficient	[21]
μ	1.8×10^{-5} Pa s	Dynamic viscosity of air	[21]
ρ	1.2 kg m ⁻³	Density of air	[21]
λ	0.5	Average number of exhaled IAs per breath	[22]
I	360	Number of breaths of IP	
$p_a p_v$	0.1	Channel transmission probability	

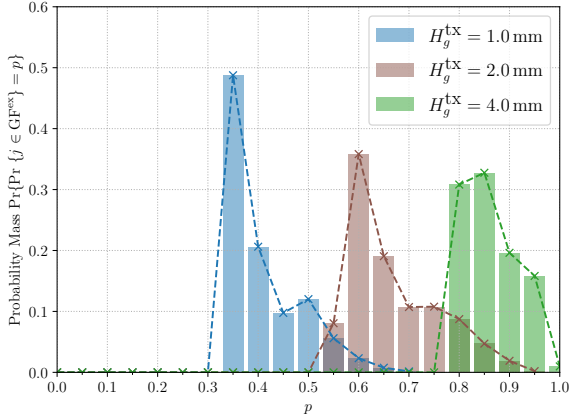


Figure 2: Empirical distribution of the probability that an IA passes through the gap at IP's face mask during exhalation for different gap heights H_g^{tx} .

6.2 Leakage at IP's Face Mask

First, we examined how the fit of the face mask of the IP impacts the probability that an exhaled IA passes through the gap. To this end, we drew 5000 random exhalation times according to (2) and computed the respective random probabilities that particles exhaled at these time instants are part of the gap flow GF^{ex} , cf. (5).

In Fig. 2, we show the empirical frequencies of these probabilities after binning them into bins of width 0.05 for different gap heights H_g^{tx} . We observe from Fig. 2 that the mean probability for an exhaled particle to escape through the gap increases as we increase H_g^{tx} . Furthermore, we observe that the random escape probabilities spread considerably. For example, for the default parameter setting from Table 1 shown in blue in Fig. 2, the escape probabilities are spread over the interval $[0.35; 0.65]$. In Fig. 3, the empirical frequencies of the escape probabilities are shown as box plots. In this representation, we can directly compare the distributions of the escape probabilities for different values of H_g^{tx} . In particular, we observe from Fig. 3 that the spread of the empirical escape probabilities is relatively large for $H_g^{\text{tx}} = 1$ mm and $H_g^{\text{tx}} = 2$ mm and decreases only for $H_g^{\text{tx}} = 4$ mm as in this case almost all particles escape through the gap.

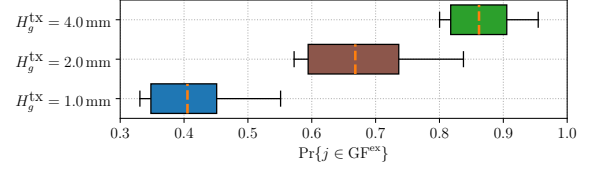


Figure 3: Empirical distribution of the probability that an IA passes through the gap at IP's face mask during exhalation for different gap heights H_g^{tx} . The orange dashed lines indicate the empirical mean value. The left and right ends of the boxes indicate the third and first quartile, respectively. The left and right whiskers end at the 95% and the 5% quantile, respectively.

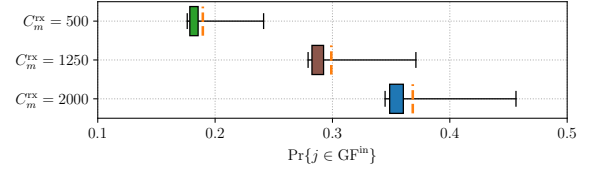


Figure 4: Empirical distribution of the probability that an IA passes through the gap at HP's face mask during inhalation for different viscous porous resistances C_m^{rx} . The orange dashed lines indicate the empirical mean value. The left and right ends of the boxes indicate the third and first quartile, respectively. The left and right whiskers end at the 95% and the 5% quantile, respectively.

6.3 Leakage at HP's Face Mask

Next, we examine the randomness contributed by the splitting of the inhalation air flow into mask flow and gap flow at the HP. To this end, similar to the previous section, we drew 5000 random inhalation times according to (10) and computed the respective probabilities that an IA passes through the gap at the HP's face mask. Then, we studied the empirical distribution of these probabilities for different viscous porous resistances C_m^{rx} of the HP's face mask.

From Fig. 4, we observe that the spread of these probabilities is rather small as compared to the exhalation case, cf. Fig. 3. Furthermore, we observe from Fig. 4 that the distribution of the probabilities remains concentrated even as C_m^{rx} decreases, i.e., in very different regimes. Indeed, this observation is plausible given that the inhalation flow as determined by (9) exhibits a smaller dynamic range than the exhalation flow, cf. Fig. 1. One important conclusion we draw from the observations in this section and the previous section is that the average flow velocity is not a sufficient indicator for the assessment of the filtration efficiency of an imperfectly fitted face mask if the actual air flow pattern exhibits dynamics beyond constant.

6.4 Impact of IP's Face Mask on IIA Statistics

Finally, we examined the impact of the fit of the face mask of the IP on the number of inhaled infectious aerosols IIA as defined in (18). From the cumulative empirical distribution of the RV IIA shown in Fig. 5, we observe that the infection probability, as defined in (19), is highly sensitive towards changes in H_g^{tx} for infectious doses θ ranging from 2 to 12 particles. However, for larger infectious doses, i.e., $\theta \gg 12$, the impact of H_g^{tx} on the infection probability is rather small. This is an interesting observation as it shows the power of the proposed model for identifying the regime in which the infection risk is sensitive to the fit of the IP's face mask.

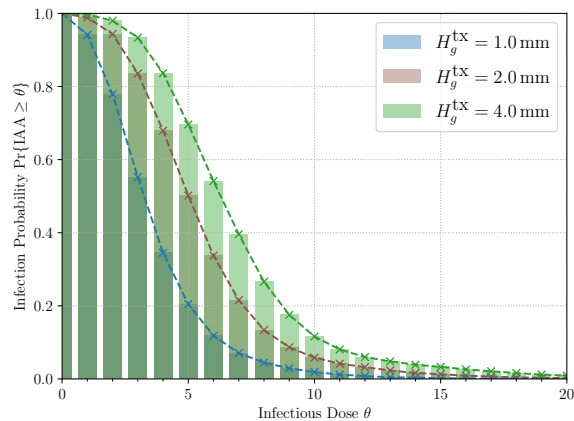


Figure 5: Cumulative empirical distribution of number of inhaled infectious aerosols IAA for different gap heights of IP's face mask.

7 CONCLUSIONS

In this paper, we presented a novel model for the impact of imperfectly fitted face masks on airborne virus transmission based on the MC paradigm. By formulating the problem of virus transmission as a communication problem, we obtained a statistical virus transmission model which reveals the impact of several physical face mask parameters on the virus transmission. The proposed model is simple but extends existing models by encompassing the randomness of the emission and the inhalation of IAs due to the imperfectly fitted face masks of the IP and the HP, respectively. With the help of our model, we could demonstrate the importance of the air flow dynamics for the assessment of the filtration efficiency of face masks. This observation is especially relevant as virus transmission prevention concerns foremost random (transmission) events with low probability, i.e., statistical outliers, and, hence, risk assessment beyond first-order statistics is required. Finally, we have demonstrated how the proposed model can be used to characterize the end-to-end transmission of IAs from an IP to an HP statistically when both individuals wear imperfectly fitted face masks. In the broader context of MC, our model provides a step towards understanding how the stochastic variability of the signaling molecules, which are commonly assumed to be identical, may impact the statistics of the end-to-end communication channel.

Possible extensions of the work presented in this paper include a more comprehensive modeling of the physical environment in which the virus transmission takes place and the validation of the proposed model with empirical data.

REFERENCES

- [1] Parham Azimi et al. 2021. Mechanistic transmission modeling of COVID-19 on the Diamond Princess cruise ship demonstrates the importance of aerosol transmission. *Proc. Natl. Acad. Sci. U.S.A* 118, 8 (Feb. 2021). <https://doi.org/10.1073/pnas.2015482118>
- [2] Michael Taynnan Barros et al. 2020. Molecular Communications in Viral Infections Research: Modelling, Experimental Data and Future Directions. arXiv:2011.00002 [q-bio.OT] <https://arxiv.org/abs/2011.00002>
- [3] Rajesh K. Bhagat, M. S. Davies Wykes, Stuart B. Dalziel, and P. F. Linden. 2020. Effects of ventilation on the indoor spread of COVID-19. *J. Fluid Mech.* 903 (Nov. 2020), F1. <https://doi.org/10.1017/jfm.2020.720>
- [4] Y. Chahibi and I. F. Akyildiz. 2014. Molecular Communication Noise and Capacity Analysis for Particulate Drug Delivery Systems. *IEEE Trans. Commun.* 62, 11 (Nov. 2014), 3891–3903.
- [5] Yafang Cheng et al. 2020. Distinct regimes of particle and virus abundance explain face mask efficacy for COVID-19. *medRxiv* (2020). <https://doi.org/10.1101/2020.09.10.20190348>
- [6] Luc Devroye. 1986. General principles in random variate generation. In *Non-uniform Random Variate Generation* (1 ed.). Springer, 27–82.
- [7] Gulec Fatih and Atakan Baris. 2021. Fluid dynamics-based distance estimation algorithm for macroscale molecular communication. *Nano Commun. Netw.* 28 (Feb. 2021), 100351. <https://doi.org/10.1016/j.nancom.2021.100351>
- [8] Monica Gandhi and Linsey C. Marr. 2021. Uniting Infectious Disease and Physical Science Principles on the Importance of Face Masks for COVID-19. *Med* 2, 1 (Jan. 2021), 29–32. <https://doi.org/10.1016/j.medj.2020.12.008>
- [9] Fatih Gulec and Baris Atakan. 2020. A molecular communication perspective on airborne pathogen transmission and reception via droplets generated by coughing and sneezing. *arXiv preprint arXiv:2007.07598* (2020).
- [10] Jeremy Howard et al. 2021. An evidence review of face masks against COVID-19. *Proc. Natl. Acad. Sci. U.S.A* 118, 4 (Jan. 2021). <https://doi.org/10.1073/pnas.2014564118>
- [11] Ben Hu, Hua Guo, Peng Zhou, and Zheng-Li Shi. 2021. Characteristics of SARS-CoV-2 and COVID-19. *Nat. Rev. Microbiol.* 19, 3 (Mar. 2021), 141–154. <https://doi.org/10.1038/s41579-020-00459-7>
- [12] M. Khalid, O. Amin, S. Ahmed, B. Shihada, and M. Alouini. 2019. Communication through Breath: Aerosol Transmission. *IEEE Commun. Mag.* 57, 2 (Feb. 2019), 33–39. <https://doi.org/10.1109/MCOM.2018.1800530>
- [13] M. Khalid, O. Amin, S. Ahmed, B. Shihada, and M. S. Alouini. 2020. Modeling of Viral Aerosol Transmission and Detection. *IEEE Trans. Commun.* 68, 8 (Aug. 2020), 4859–4873. <https://doi.org/10.1109/TCOMM.2020.2994191>
- [14] Caglar Koca, Meltem Civas, Selin M. Sahin, Onder Ergonul, and Ozgur B. Akan. 2021. Molecular Communication Theoretical Modeling and Analysis of SARS-CoV2 Transmission in Human Respiratory System. (2021). arXiv:2011.05154 [physics.bio-ph] <https://arxiv.org/abs/2011.05154>
- [15] Zhipeng Lei, James Yang, Ziqing Zhuang, and Raymond Roberge. 2012. Simulation and Evaluation of Respirator Face Seal Leaks Using Computational Fluid Dynamics and Infrared Imaging. *Ann. Occup. Hyg.* 57, 4 (12 2012), 493–506. <https://doi.org/10.1093/annhyg/mes085>
- [16] Jos Lelieveld et al. 2020. Model Calculations of Aerosol Transmission and Infection Risk of COVID-19 in Indoor Environments. *Int. J. Environ. Res. Public Health* 17, 21 (Nov. 2020). <https://doi.org/10.3390/ijerph17218114>
- [17] Rajat Mittal, Charles Meneveau, and Wen Wu. 2020. A mathematical framework for estimating risk of airborne transmission of COVID-19 with application to face mask use and social distancing. *Phys. Fluids* 32, 10 (Oct. 2020), 101903. <https://doi.org/10.1063/5.0025476> arXiv:https://doi.org/10.1063/5.0025476
- [18] Rajat Mittal, Rui Ni, and Jung-Hee Seo. 2020. The flow physics of COVID-19. *J. Fluid Mech.* 894 (Mai 2020), F2. <https://doi.org/10.1017/jfm.2020.330>
- [19] Lidia Morawska and Donald K Milton. 2020. It Is Time to Address Airborne Transmission of Coronavirus Disease 2019 (COVID-19). *Clin. Infect. Dis.* 71, 9 (Nov. 2020), 2311–2313. <https://doi.org/10.1093/cid/cia939>
- [20] Tadashi Nakano, Andrew W. Eckford, and Tokuko Haraguchi. 2013. *Molecular Communication* (1 ed.). Cambridge University Press. <https://doi.org/10.1017/CBO9781139149693>
- [21] Robinson Perić and Milovan Perić. 2020. Analytical and numerical investigation of the airflow in face masks used for protection against COVID-19 virus—implications for mask design and usage. *J. Appl. Fluid Mech.* 13, 6 (Nov 2020), 1911–1923.
- [22] Michael Riediker and Dai-Hua Tsai. 2020. Estimation of Viral Aerosol Emissions From Simulated Individuals With Asymptomatic to Moderate Coronavirus Disease 2019. *JAMA Netw. Open* 3, 7 (Jul. 2020), e2013807–e2013807. <https://doi.org/10.1001/jamanetworkopen.2020.13807>
- [23] Jackie Sue Russo and Ezzat Khalifa. 2011. Computational study of breathing methods for inhalation exposure. *HVAC&R Res.* 17, 4 (Aug. 2011), 419–431. <https://doi.org/10.1080/10789669.2011.578701> arXiv:https://www.tandfonline.com/doi/pdf/10.1080/10789669.2011.578701
- [24] Max Schurwanz, Peter Adam Hoehner, Sunasheer Bhattacharjee, Martin Dammrath, Lukas Stratmann, and Falko Dressler. 2020. Duality between coronavirus transmission and air-based macroscopic molecular communication. (2020). <https://arxiv.org/abs/2009.04966>
- [25] I. M. Viola et al. 2021. Face Coverings, Aerosol Dispersion and Mitigation of Virus Transmission Risk. *IEEE Open J. Eng. Med. Biol.* 2 (Jan. 2021), 26–35. <https://doi.org/10.1109/OJEMB.2021.3053215>
- [26] W. Joost Wiersinga, Andrew Rhodes, Allen C. Cheng, Sharon J. Peacock, and Halie C. Prescott. 2020. Pathophysiology, Transmission, Diagnosis, and Treatment of Coronavirus Disease 2019 (COVID-19): A Review. *JAMA* 324, 8 (Aug. 2020), 782–793. <https://doi.org/10.1001/jama.2020.12839>